# Collimation of Acoustic Waves: Experimental and Computational Verification

C. Kohnle
*Physics and Astronomy Department, College of Charleston*
(Dated: May 17, 2024)

Recently, the collimation of sound waves has become increasingly studied, due to the benefits of applications of devices which use this effect. Much of the current work in this field is done within the ultrasonic ranges, which is useful for applications like imaging and materials testing. This paper explores a method of collimating acoustic range sound waves with spherical reflectors. An obvious benefit of working within the acoustic range is the possibility of using these collimated waves to interfere significantly with other acoustic range sound. We collimate a source of 400 Hz sound waves with a parabolic reflector with a radius of 15.5 in. We measure the amplitude of the pressure waves at 70 points distributed radially behind the source, where we expect to see collimation. We create a Lagrangian simulation of sound waves propagating through air. This is done with the purpose of simulating the physical setup that we took measurements for. We then compare the two measurements produced by each method at the same positions and find an average percent difference of $3.6 \pm 0.2\%$. With this, we conclude that our simulation reasonably replicates the behavior that we are interested in. We use this to take advantage of the increased resolution and ease of working with simulations to find a post-focal degree of collimation of $0.05 \pm 0.002^\circ$ within the 125 cm region behind the sound source.

## I. INTRODUCTION

### Motivation

Recently, the collimation of sound waves has become increasingly studied, due to the benefits in application of devices which use this effect. Much of the current work in this field is done within the ultrasonic ranges, which is useful for applications like imaging and materials testing. We will briefly explore the benefits of collimating acoustic range sound waves.

An obvious benefit of working within this range is the possibility of using these collimated waves to interfere meaningfully with other acoustic range sound. Because of this, I would like to create a device capable of collimating acoustic sound and determine how such a device can be used to interfere, and particularly dampen, external sources of acoustic sound.

This overarching project will be spread among multiple papers, with this being the first. We will explore a possible method of collimating acoustic range sound in order to later determine how such a setup could be used to dampen acoustic sources external to it. We create our setup using existing theory about wave reflection from parabolic surfaces to collimate some of the sound from a speaker. We will verify this collimation both experimentally and computationally. Later, this setup will be used in further papers within the overarching project to interfere with external sound sources.

### Theory

The amplitude of a sound wave in a medium is understood as the pressure difference caused by that sound wave, called the acoustic pressure. This differs from the background environmental pressure, called the ambient pressure.

The propagation of sound waves through a medium in three dimensions is generally given by the Laplacian equation

$$\nabla^2 p - \frac{1}{c^2}\frac{\partial^2 p}{\partial t^2} = 0 \tag{1}$$

where $p$ is the acoustic pressure and $c$ is the speed of sound in the medium. This is a form of the general wave equation, making it mathematically analogous in some ways to the case of the propagation of electromagnetic waves. Crucially, the two are analogous in how they reflect off of surfaces.

The analogous optical theory that we will be making use of is the phenomenon of optical focal points from curved reflective surfaces. For our purposes a surface is "acoustically reflective" if it reflects a measurable amplitude of sound waves. For electromagnetic waves, this reflection follows the law of reflection, which states that

$$\theta_i = \theta_f \tag{2}$$

where $\theta_i$ is the incident angle of the electromagnetic wave from the normal vector of the point of contact, and $\theta_f$ is resulting the angle of reflection. According to [2] sound waves reflect identically, despite being longitudinal waves.

With this assumption, we can apply the rules of parabolic reflection to acoustic waves. According to photonics, if the reflector has a small curvature compared to the distances involved

$$\frac{1}{f} = \frac{1}{d_o} + \frac{1}{d_i} \tag{3}$$

holds true, where $f$ is the focal point of the reflector, $d_o$ is the distance of the object to the mirror and $d_i$ is

the visual distance of the image. This formula assumes that the lens must be thin, with a small aperture. For the case of acoustic reflection, the analogous assumption is that the sound reflects from the surface of the reflector, rather than traveling some distance through it before reflecting. When the object is placed at the focal point, $d_o$ approaches $f$, and so $d_i$ necessarily approaches infinity. This is physically represented with the waves emanating from the mirror being nearly parallel with each other, and therefore forming a collimated beam.

It is useful to know the conversion formula between the sound pressure level (SPL) in decibels and the pressure difference caused by our sound wave, as SPL is how humans perceive and typically measure sound. The conversion equation for the SPL from the pressure is

$$SPL(dB) = 20 \log \frac{p}{p_r} \tag{4}$$

where $p_r$ is the reference pressure, in this case, the pressure threshold for human hearing. The SPL is a numerical description of how humans perceive the volume of sound, so it is how we will be measuring the pressure difference caused by the sound waves. Note that a difference in six decibels is about equal to the pressure measured being doubled. Our microphone uses $Z$-frequency weighting, which means that the volume that it measures it not significantly dependant on the frequency of that sound. This does not reflect how the human ear measures volume, but does make calibrating the device easier and less prone to error due to uncertainty in the frequency.

Finally, we need a metric to determine *how* collimated the resultant wave behavior is. What we mean by saying that a beam is well-collimated is that the beam does not significantly change its width with distance. In other words, as the beam travels, it does not significantly narrow or widen within the range that we are observing. In terms of quantitatively defining this collimation, we can find the semidivergence angle of the beam. This angle represents how parallel the waves that make up the beam are traveling with respect to each other. For the longitudinal waves that we expect to see, we can use the Gaussian beam formula outlined in [4]. It states that

$$\theta = \tan\left(\frac{h}{d}\right)^{-1} \tag{5}$$

where $\theta$ is the semidivergence angle of the beam, $h$ is the change in the width of the beam between two sections of the beam, and $d$ is the distance travelled to get this width change.

## II. METHODS

### A. Experimental Methods

Our experimental setup includes a speaker capable of emitting acoustic-range sound, a concave spherical dish, and a one-directional microphone. For our specific setup, we used a dish with a diameter of 31 in and a radius of curvature of 150 cm. The entire setup was built in a room which has a relatively low variant background noise. We set up the spherical dish so that the dish's focal point was horizontal to the center, with the speaker positioned at the focal point of this dish. Figure 1 shows a top-down view of this setup with the important geometric relations.

The microphone was attached to a tripod adjusted to the same height as the speaker and focal point. We also attached a filter called a windscreen to the microphone which should prevent turbulence or currents in the air from introducing noise into our experimental results. The microphone was connected to an IPhone X, which was running an app called dB meter to record the peak volume in decibels. It is important to make sure that the space around the setup is clear of any high-density objects. Any dense (denser than air) objects will significantly absorb or reflect sound waves, introducing uncertainty into our measurements. For our setup, we were unable to entirely eliminate dense objects, as we needed a stand to hold up our sound source so that it would be level with the dish's focal point. We make the assumption that this had a negligible effect on our data, as the stand has a surface area which is small compared to the surface of the sound source. Since the two are necessarily next to each other, and we have already assumed that the sound source's size has a negligible affect on the SPL measurements, we can couple these assumptions together. To be clear, an uncertainty is introduced here, but we assume that it is small enough to neglect within the goals of this experiment. The discussion section will address how these uncertainties could be minimized in the future, under future experiments where the uncertainty in the SPL measurements is more important to the conclusion of the experiment.

First, before turning on the speaker, we move the microphone around the two meter radius circle surrounding the speaker. 20 measurements are taken at random points within this circle and then the average is taken. This is done to get a general background measurement of the noise level in the room. In theory, the volume of the background sound depends on the position of the microphone, but since the standard deviation of these measurements is very low, we can approximate that it is uniformly the mean everywhere which we will be measuring.

Next, we turn on the speaker to 400 Hz. This particular frequency was chosen due to it being within the auditory range, and particularly in the range that humans associate most with music and speech. A meter stick and protractor are used to subdivide the two meter

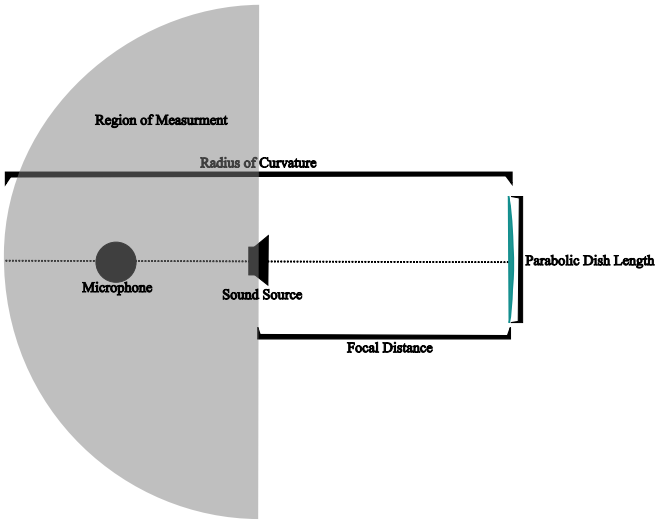


FIG. 1. The figure shows a top-down view of our experimental setup. For our setup, the radius of curvature is $R = 150$ cm, the focal distance is $d_f = 75$ cm, and the parabolic dish length is $l = 31$ in. The region highlighted in grey is the region around which we have spread our 70 measurements, according to the methods defined in the body of the text. The microphone was placed at each of these 70 points.

radius around the speaker into a polar grid with 7 angular ticks $\theta$ of 30° each and 10 radial ticks $r$ of 20 cm, beginning at $r = 20$ cm. The microphone is moved to each of these points by the experimenter, who then leaves the setup area, as to not affect the sound wave propagation with their body. When they return, the software displays the average volume measured during that time, and the uncertainty in their measurement. For most of the measurements, our uncertainty was within a decibel, so for the remainder of the experiment we assume that the uncertainty in our experimental results is ±1‘dB. A measurement is taken with the same process for every unique point within the polar grid and recorded.

Finally, the parabolic dish is removed from the setup and another set of measurements is taken the exact same way as during the last set. This is meant to gauge the propagation of sound from the specific speaker that we use, without external obstacles, such as the dish. With this measurement, we provide a baseline, allowing us to make quantitative comparisons between our dished setup and our non-dished setup.

### B. Computational Methods

The simulation employed in this experiment aims to replicate the behavior of acoustic waves propagating through a uniform-temperature, non-dynamic medium. Modeled as a Lagrangian simulation, it tracks individual wave-particle objects throughout their time-evolution within the system. This approach contrasts with non-Lagrangian simulations, where the system's values at each coordinate are pre-solved and then displayed, lacking the detailed tracking of individual wave entities. Specifically, the simulation is set on a rectangular 400 by 400 coordinate grid, which physically represents the 400cm by 400cm plane over which we took the experimental measurements, with the speaker centered at $(200, 200)$. The simulation creates wave objects that contain information about their pressure amplitude, phase shift, frequency, direction and other important physical properties. They are continuously created at the point $(200, 200)$, and uniformly spherically propagate away from the source. The simulation uses small difference time-integration to evolve these waves through time. These waves can interact with obstacles, which are placed onto the coordinate grid. They reflect off these obstacles with perfect efficiency, at the angle described by Equation 2. The images created by the simulation are made by calculating the pressure at each point, as contributed by each of these wave objects. By simulating the time-evolution of individual wave-particle objects, the simulation offers flexibility in incorporating additional elements, such as the parabolic dish used in the experiment. Unlike non-Lagrangian simulations, which struggle with the numerical generalization of additional objects' contributions to the coordinate solution, the Lagrangian approach seamlessly accommodates such additions.

Considerations for diffraction of waves by the medium are included in the simulation, aligning with well-established principles governing sound propagation through air. The simulation generates visual outputs representing the spatial distribution of acoustic pressure, with high-pressure regions depicted in red and low-pressure regions in blue. Figure 2 shows such an image.

The simulation's fidelity and accuracy are crucial for its utility in replicating experimental conditions. Validation of the simulation's accuracy involves comparison with experimental measurements obtained under identical conditions. We analyze the simulation's accuracy to the experimental results quantitatively by finding the average percent difference between the corresponding experimental and computational results.

Once we have shown that the simulation reasonably reproduces our experimental findings, we can use the simulation to determine how collimated the beam is. The simulation's high resolution and precision offer advantages over experimental methods, facilitating detailed analysis and exploration of parameters such as the degree of collimation. Leveraging these benefits, the simulation aids in determining crucial parameters, such as the post-focal degree of collimation, which may be challenging to ascertain solely through experimental means due to limitations in recording equipment.

## III. RESULTS

The results of the experimental measurements are shown in Figures 3 and 4. As expected, the volume ap-

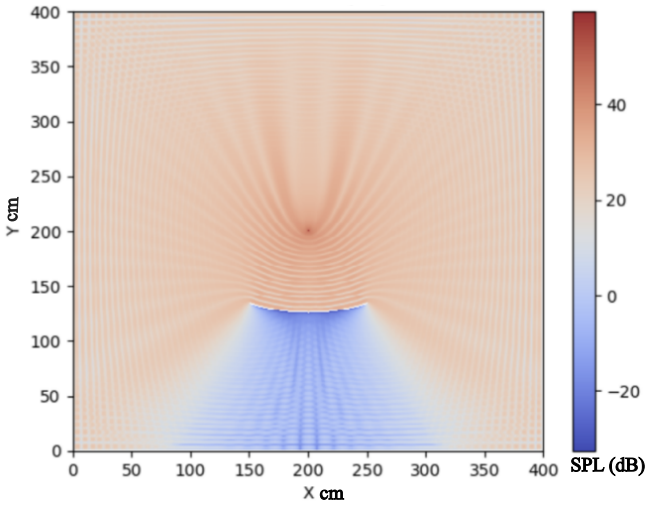


FIG. 2. The figure shows a top-down view of our simulation running with the presence of the dish. The red points represent points of high pressure, and the blue represent low pressure. There is consideration given to diffraction of waves by the medium, according to the well-studied behavior of sound through air. This simulation uses a source of 60 dB for better visual clarity.

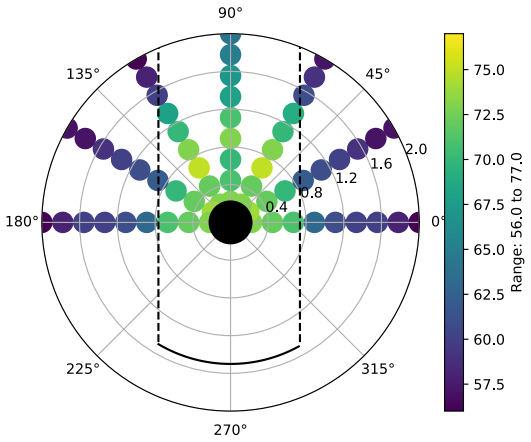


FIG. 3. The figure shows a top-down view of our experimental setup with the parabolic dish in place. The black curve is the dish, and the black dotted lines represent where we expect to see collimation. The $z$-scale represents the SPL measured at that point in decibels. The volume appears to be greater within the region of expected collimation.

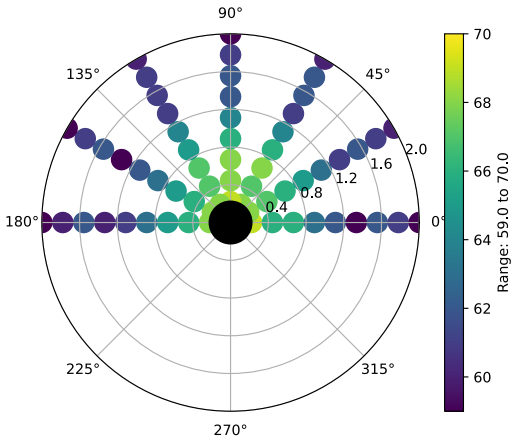


FIG. 4. The figure shows a top-down view of our experimental setup without the parabolic dish. The $z$-scale represents the SPL volume measured at that point in decibels. The volume appears to be behaving according to the anticipated inverse-square law.

pears to always be greater within the the region of expected collimation for Figure 3. The data represented in Figure 4 also behaves as expected, appearing to weaken in volume according to the inverse-square law. This can be qualitatively shown by the visible lack of change between the points who have an angular difference, but no radial difference.

We also include an additional plot in Figure 5, which shows the difference of the data points from Figures 3 and 4. Each point in Figure 5 is calculated by taking the SPL at the point given in Figure 3, and subtracting it by the SPL given in figure 4. This is beneficial to include, as we expect to see that the points within the beam radius have a greater difference in their measurements, while those outside are expected to have a more minimal, or even negative difference, which is exactly what we see. We expect to see this because

Figure 6 shows the measurements from the corresponding points in the simulation. To better reflect how our physical microphone measures the sound around it, each measurement is the average of all of the SPL values given by the simulation within a 2 cm radius around the point being measured. This radius was chosen because it is close to the length of the microphone that we used to get our experimental results. Figure 7 shows the difference between Figures 3 and 6, in order to find how much the computational approximation varies from our experimental results. Additionally, Figure 7 allows us to see roughly where our simulation doing a poorer job at replicating the experimental data.

We use our simulation software to recreate the physical setup of the experiment. Figure 5 shows a frame of this animation, but a link to the entire animation is included in Appendix A. Using this simulation to calculate the SPL at the same points as Figures 2-4, we created Figure 6.

The average percent difference between the measurements in Figures 3 and 6 is a representation of how well our simulation is approximating our experimental setup. This is plotted in Figure 7. We calculate an average percent difference of 3.6%, which suggests that our approximation is accurate for these conditions. Furthermore, we can see that the simulation tends to predict lower

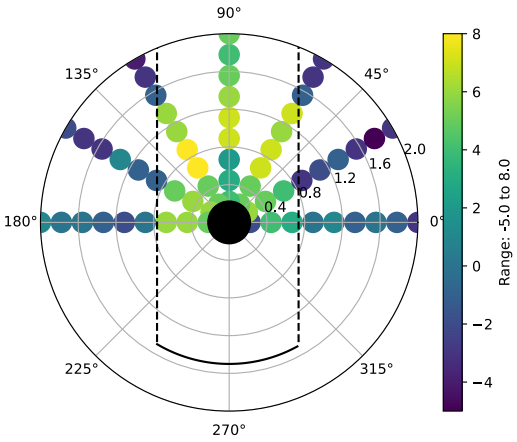


FIG. 5. The figure shows a top-down view of our experimental setup with the difference between the results represented in Figure 3 minus the results represented in Figure 4. This includes considerations of uncertainty, which was always applied in such a way as to reduce apparent collimation (i.e. making the differences outside of the region of expected collimation greater, and those inside smaller). The black curve is the dish, and the black dotted lines represent where we expect to see collimation. The $z$-scale represents the difference in SPL measured at that point in decibels. As expected, we see greater differences within the region of expected collimation.

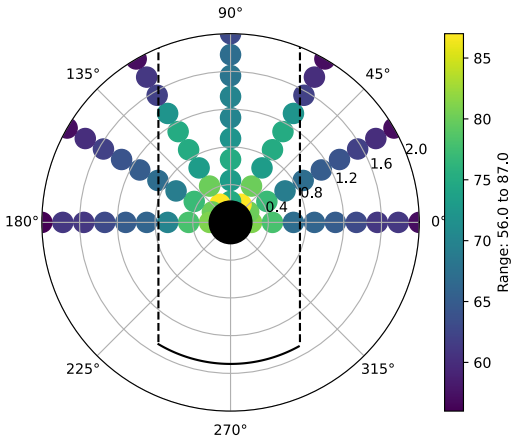


FIG. 6. This is a recreation of Figure 2 with data collected from the simulation script. The $z$-scale represents the average SPL values measured in the two-pixel radius around that point in decibels. Due to the higher SPL value bounds from measuring the SPL closer to the source, it is harder to qualitatively see evidence of collimation. This is offset by Figure 7, which implies that the computational data is roughly as collimated as the experimental analog represented in Figure 3.

SPL values close to the sound source than are actually measured. This discrepancy will be explored further in the discussion of this paper. Since we see less error at the points farther behind the source, which is where we would like to measure the beam collimation, we can use the average difference between the computational and experimental results as a good estimate of the uncertainty in our computational results.

For the purpose of evaluating the collimation of the simulated acoustic beam, we use the low percent difference between the simulation and our experimental setup at as justification to use the higher-resolution and more precise simulation results to determine the angle of collimation.

[1] outlines computational methods for simulating sound wave propagation through means of Lagrangian simulations. In an auxiliary of their paper, the authors show an animation of a short burst of acoustic waves being uniformly and spherically emitted from the focal point of a parabolic reflector. Figure 8 shows a frame of this animation, with arrows showing the direction of wave propagation for clarity. This simulation varies from our simulation in that it shows the behavior of only a small pulse of sound waves being emitted from the source. As Figure 8 shows, the region behind the source is affected by two distinct parts of each wave pulse: the spherically-propagating initial pulse, and the collimated secondary pulse. Relating this to our simulation, by continuously emitting waves, rather than a pulse, we expect that the region behind the source will be comprised of the superposition of both of these waves. The result of this, it that we do not strictly see collimation, rather we see "jets" which are the result of summing the longitudinal collimation waves with the spherical-dependence of the non-reflected sound waves. We can eliminate these cumbersome spherically-propagating wave components by restricting the emission of waves from the simulated source to only the directions that will result in those waves being reflected. It is important to note that this is not what we experimentally measured, but that this is the collimation that we are looking to prove the existence of. This is what we refer to as the "post-focal beam", as it is the beam comprised of only the sound waves which have been reflected and passed the focal point of the reflector.

The beam shown in our simulation is translational, meaning that it can be described using the well-studied mathematics of Gaussian beams. In particular, we use Equation 5 to determine the semidivergence angle of the Gaussian beam collimation. Doing so for the simulation shown in Figure 9, we find our beam to have a semidivergence angle of $0.05 \pm 0.002°$.

### A. Discussion

The small deviation that we see from perfect collimation in our computational results could be from a number of possible sources. The simulation, notably, does not include physical uncertainties that would be present in the

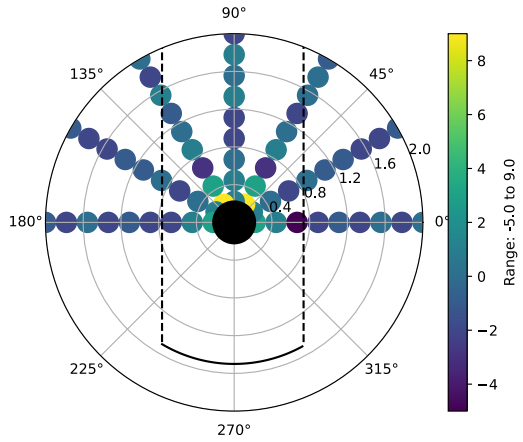


FIG. 7. The figure shows a top-down view of our experimental setup with the difference between the results represented in Figure 3 minus the results represented in Figure 4. This includes considerations of uncertainty, which was always applied in such a way as to reduce apparent collimation (i.e. making the differences outside of the region of expected collimation greater, and those inside smaller). The black curve is the dish, and the black dotted lines represent where we expect to see collimation. The $z$-scale represents the difference in SPL measured at that point in decibels. The average percent error between the two figures is $3.6 \pm 0.2\%$. Additionally, the average percent difference of the 14 values closest to the sound source is 5.5%.

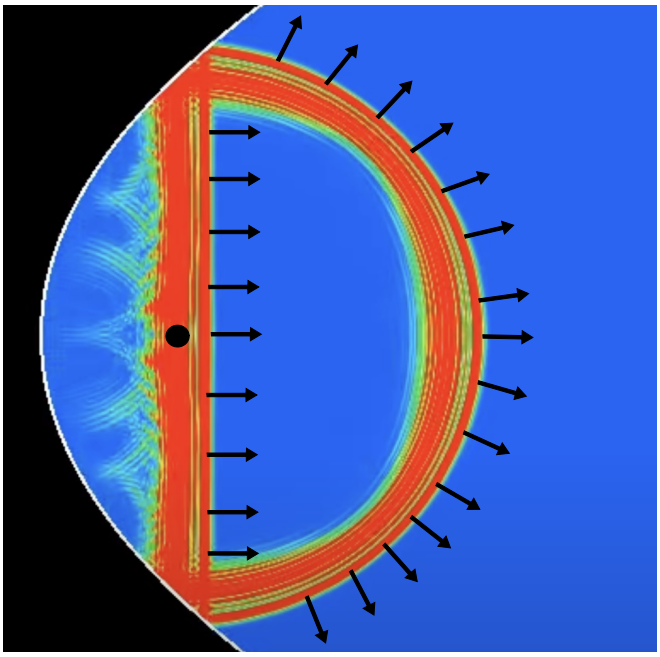

FIG. 8. Annotated frame of the animation from [1]'s simulation of acoustic pulse propagation from parabolic reflectors. The arrows represent the direction in which the waves are propagating, and the circle represents where the spherical wave source was placed. This simulation clearly shows parallel collimation from the reflected waves, but also the spherical propagation of the waves which were not reflected.

experimental analog, such as uncertainty in the shape of the reflector, the efficiency of the reflector, the amplitude of the waves being emitted, etc. Because of this, we know that this deviation from perfect collimation is not due to uncertainty, but rather a physical process that is captured by the simulation. The most likely culprit is the diffraction of the sound waves as they travel through the air. The computational solution to Equation 1 requires a term $\rho$, which represents the density of the medium through which the waves are travelling. For our simulation, we use the density of air at room temperature, 1.204 Kg/m$^3$. The diffraction of waves as they travel through a medium is partially dependant on the density of that medium. Because of this effect, we expect that our simulation, if working properly, should see the wave objects spread out as they travel through the medium, even after being collimated. This is summarized by [3], who states that it is a primary reason why perfectly collimating beams in air is impossible, even in principle.

As is explained in the Introduction, this paper is one in a series, which set out to establish the theoretical basis for a device capable of collimating acoustic range sound and attenuating acoustic range sound external to it. For example, using the beam to destructively interfere with unwanted sound sources, like construction equipment or engine noise from a jet. A major advantage of using a collimated acoustic beam for interference purposes is that it can be more precisely managed than a point-source, increasing its general applicability. Because of this, we would like to collimate the beam as much as possible in future iterations of our design. Looking at Equation 4, we can improve how collimated our beam is by using a larger, parabolic sound reflector. This was not done in this experiment due to not having access to such a reflector. We could also improve the accuracy and precision of the location of our source point source. For our experimental setup, the majority of the calculated uncertainty in our SPL comes from the uncertainty in the source's position. This uncertainty is high, due to our the high ratio of our uncertainty in the source's position compared to the radius of curvature of the dish. Because of this, we can mitigate the affects of this uncertainty in future experiments with either a smaller sound source, or a less curved reflector. This will become extremely important when creating more physical setups, but does not play a significant role in our simulations, as uncertainty is not considered in our current code. Implementation of these error considerations would provide an error bound for all of the measurements shown in Figure 6, the propagation of which would arise naturally from the Lagrangian implementation of error sources. This will likely be important during further papers, perhaps one which seeks to address concerns of how manufacturing errors would affect such a device's performance. If our simulation is accurately propagating this error, the error bounds of

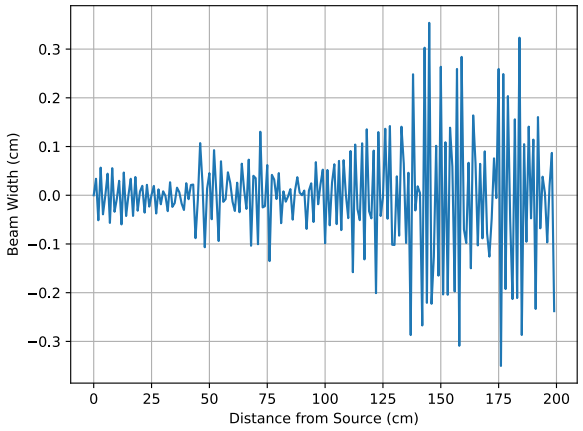


FIG. 9. The figure above shows how the beam width measured within the simulation changes as the distance behind the source increases. The variance in these values correlates to the peaks and valleys of the translational waves. From the distance of 0 to 130 cm, where the first width greater than 0.2 cm occurs, is $0.05 \pm 0.002°$.

such a simulation should include most values shown in Figure 2, as we have isolated the physical setup in such a way that minimizes the affect of other sources of error in our measurements, such as reflection from objects other than the dish and sounds from sources other than the source at the focal point. For example, we ensure that we have a relatively small dependence on the $z$-coordinate, a dependence which is not physically tracked in our simulation. Should any other systematic errors prove to be more significant than our simulation needs to consider, this would be determined in such a future paper based on this error-adjusted simulation. In future experiments, enhancements to the simulation may include the incorporation of error considerations to provide error bounds for simulated measurements. This would enable a comprehensive assessment of the simulation's performance under varying conditions, including the propagation of uncertainties arising from sources such as manufacturing errors. Such improvements would ensure the simulation's robustness and applicability in addressing broader research objectives.

Looking forward to future experiments, now that there is sufficient evidence for the collimation of acoustic waves with a spherical reflector, and we have created a computational simulation capable of accurately reproducing this collimation, then next goal of the overarching project that includes this paper will be to determine how well these acoustic beams can be used to attenuate sound from external sources. The next paper in particular will explore how the incident angle, relative phase shift, and frequency differences between the collimated and external sound sources will affect how well the resultant sound can be attenuated. This is all done with the end goal of creating a setup which has been optimized for attenuating the maximum amount of external sound. We anticipate that there will be a high dependence on the frequency difference between the two sound sources and how well they attenuate each other, so we also have a secondary experiment in mind which will create a setup capable of automatically changing what frequency the collimated acoustic beam utilizes, according to what frequency of external sound must be attenuated out. Overall, this paper has both accomplished its original purpose of creating a setup which collimates acoustic-range sound waves, but also has resulted in the creation of simulation software which will help with setup optimization for the remainder of the project. Crucially, it will allow us to test the theoretical effectiveness of different setups without the associated costs of physically building them.

## IV. CONCLUSION

We collimate a source of 400 Hz sound waves with a parabolic reflector with a radius of 15.5 in. We measure the amplitude of the pressure waves at 70 points distributed radially behind the source, where we expect to see collimation. We create a Lagrangian simulation of sound waves propagating through air. We then compare the two measurements that both methods retrieved at the same positions and find an average percent difference of $3.6 \pm 0.2\%$. With this, we conclude that our simulation reasonably replicates the behavior that we are interested in. We use this to take advantage of the increased resolution and ease of working with simulations to find a post-focal degree of collimation of $0.05 \pm 0.002°$.

[1] Hans Petter Langtangen. *Finite difference methods for wave equations*. CC Attribution 4.0 license, 2016.
[2] Bilkent Samsurya. Realtime audio raytracing and occlusion in csound and unity. 2022.
[3] Xometry. Collimated beam: Definition, how it works, applications, and benefits. *Xometry.com*, 2023.
[4] Yurii Zubov. Long-range nonspreading propagation of sound beam through periodic layered structure. *Nature*, 2020.